Asociación Argentina
de Mecánica Computacional

Mecánica Computacional Vol XXVI, pp.3005-3018
Sergio A. Elaskar, Elvio A. Pilotta, Germán A. Torres (Eds.)
Córdoba, Argentina, Octubre 2007

DYNAMIC ANALYSIS OF CONSTRAINED NONLINEAR MULTIBODY SYSTEMS WITH INTERMITTENT CONTACT

Elisabet Lens[a] **and Alberto Cardona**[b]

[a]*SAMTECH Ibérica, c/València 230, 08012 Barcelona, España, lisa.lens@samcef.com,*
http://www.samcef.com
[b]*Centro Internacional de Métodos Computacionales en Ingeniería, CIMEC-INTEC,*
Conicet-Universidad Nacional del Litoral, Güemes 3450, 3000 Santa Fe, Argentina,
acardona@intec.unl.edu.ar

Keywords: Energy Preserving Schemes, Multibody Systems Dynamics, Impact.

Abstract. The present work deals with the dynamic analysis of flexible, nonlinear multibody systems undergoing intermittent contact. The contact event is assumed of finite duration and the contact forces are computed during the simulation. Two kinds of contacts are considered: rigid contact condition, treated by using the slack variable technique, and flexible contact, treated by using suitable phenomenological laws that relate the contact forces and the inter-penetration between bodies. The work is developed within the framework of an energy preserving time integration scheme, that provides unconditional stability for the kind of systems analyzed in this work.

1 INTRODUCTION

Intermittent contact can occur between two rigid or deformable bodies of the system or with an external body. The nature of the contact can be accidental, as the impact of a member of the system on an unexpected obstacle. Another source of intermittent contact are the clearances in the joints of multibody systems, due to manufacturing imperfections or damage. Sometimes intermittent contact is an inherent feature of the system, as in the case of cam-follower systems. The various approaches to the modelling of unilateral contact fall into two main categories, depending on the assumed duration of the contact, as mentioned by Bottasso and Trainelli (Bottasso and Trainelli, 2001) and Bauchau (Bauchau, 2000).

The first approach (Impulsive Model) considers null the duration of the contact. The configuration of the system is assumed to be identical before and after impact and an appropriate model is used for relating both states. This approach was first proposed by Kane (Kane, 1962) and extended by Khulief and Shabana (Khulief and Shabana, 1986) taking into account the flexibility of system components. There are two alternatives to this theory: Newton's method that relates the relative normal velocities of the contacting bodies using an appropriate restitution coefficient, and Poisson's method (Pfeiffer and Glocker, 1996) that divides the impact in two phases: an initial compression phase brings the normal relative velocity of the bodies to zero through the application of an impulse at the contact location; then an expansion phase applies an impulse of opposite sign which magnitude is related to the magnitude of the first impulse through a restitution coefficient.

This first approach requires the implementation of an algorithm for exact detection of the time instant in which the impact event is produced, at which the time integration scheme has to be stopped and the impulse magnitude is computed modifying the velocities. Several alternatives have been proposed to this end. This strategy can be time consuming and complicated in the case of multiple impacts, as it may happen when modelling impact between flexible bodies in contact or between several rigid bodies.

In the second approach (Continuous Model) the duration of the impact is assumed finite and the time history of the forces acting between the bodies in contact (which can be rigid or flexible) is explicitly computed at the simulation. This is achieved by introducing a suitable phenomenological model for the contact forces, usually expressed as functions of the approach between the contact bodies. As for all the contact models we have a complementary problem: either the sum of the relative distance and the approach is greater that zero (the contact forces vanish), or the same sum is null and the relative distance is equal and opposite to the approach (inter-penetration with non-vanishing interaction forces).

In this work the contact event is assumed to be of finite duration. Two different approaches are used to model the intermittent contact: rigid and flexible impact. In the case of the rigid impact, the unilateral contact condition is transformed into a holonomic constraint by using a slack variable. In the case of flexible impact, a simple model that relates contact forces with the inter-penetration between bodies is used. Both approaches are used to analyze the impact between rigid and flexible bodies and compared, establishing which one is the best choice for each case.

2 FORMULATION OF THE PROBLEM

Let us describe a conservative mechanical system in terms of N generalized coordinates $\boldsymbol{q}$ submitted to R algebraic constraints

$$\boldsymbol{\Phi}(\boldsymbol{q}) = \boldsymbol{0}. \tag{1}$$

Its dynamic properties can be derived from an appropriate description of the potential energy of the system $\mathcal{V} = \mathcal{V}(\boldsymbol{q})$ and of its kinetic energy, which can be put in quadratic form without loss of generality

$$\mathcal{K} = \frac{1}{2}\boldsymbol{v}^T \boldsymbol{M} \boldsymbol{v}. \tag{2}$$

The $(M \times M)$ inertia matrix $\boldsymbol{M}$ can be assumed constant, symmetric and positive definite since velocities $\boldsymbol{v}$ are expressed in a *material frame*. The latter are treated as quasi-coordinates and thus take the form of linear combinations of generalized coordinate time derivatives

$$\boldsymbol{v} = \boldsymbol{L}(\boldsymbol{q})\dot{\boldsymbol{q}}, \tag{3}$$

$\boldsymbol{L}(\boldsymbol{q})$ being a $(M \times N)$ matrix with $M \leq N$. This inequality covers the case in which the description of angular velocities is made in terms of redundant rotation parameters such as Euler parameters. In this case the redundancy between parameters has to be removed by adding appropriate constraints to the global set (1).
The motion equations result from the application of Hamilton's principle:

$$\delta \int_{t_1}^{t_2} \left\{ \frac{1}{2}\boldsymbol{v}^T \boldsymbol{M} \boldsymbol{v} - \boldsymbol{\mu}^T \left(\boldsymbol{v} - \boldsymbol{L}(\boldsymbol{q})\dot{\boldsymbol{q}}\right) - \mathcal{V}(\boldsymbol{q}) - \boldsymbol{\lambda}^T \boldsymbol{\Phi}(\boldsymbol{q}) \right\} dt = 0 \tag{4}$$

We successively perform variations on the variables $\boldsymbol{\mu}$, $\boldsymbol{\lambda}$, $\boldsymbol{v}$ y $\boldsymbol{q}$:

- the variation of the multipliers $\boldsymbol{\mu}$ restores the velocity equations (3)
- variation of the multipliers $\boldsymbol{\lambda}$ restores the constraints set (1)
- the variation of the velocities $\boldsymbol{v}$ shows that the multipliers $\boldsymbol{\mu}$ have the meaning of generalized momenta

$$\boldsymbol{\mu} = \boldsymbol{M}\boldsymbol{v} \tag{5}$$

- the variation of the generalized displacements $\boldsymbol{q}$ yields

$$\int_{t_1}^{t_2} \left\{ \delta \boldsymbol{q}^T \left(-\frac{\partial \mathcal{V}}{\partial \boldsymbol{q}} - \frac{\partial \boldsymbol{\Phi}^T}{\partial \boldsymbol{q}}\boldsymbol{\lambda} + \frac{\partial}{\partial \boldsymbol{q}} \left[(\boldsymbol{L}\dot{\boldsymbol{q}})^T \boldsymbol{\mu} \right] \right) + \delta \dot{\boldsymbol{q}}^T \boldsymbol{L}^T \boldsymbol{\mu} \right\} dt = 0 \tag{6}$$

  from which the dynamic equilibrium equations will be extracted.

Integration by parts of (6) yields

$$\left[\delta \boldsymbol{q}^T \boldsymbol{L}^T \boldsymbol{\mu}\right]_{t_1}^{t_2} + \int_{t_1}^{t_2} \delta \boldsymbol{q}^T \left\{ -\frac{\partial \mathcal{V}}{\partial \boldsymbol{q}} - \frac{\partial \boldsymbol{\Phi}^T}{\partial \boldsymbol{q}}\boldsymbol{\lambda} + \frac{\partial}{\partial \boldsymbol{q}} \left[(\boldsymbol{L}\dot{\boldsymbol{q}})^T \boldsymbol{\mu} \right] - \frac{d}{dt}\left(\boldsymbol{L}^T \boldsymbol{\mu}\right) \right\} dt = 0 \tag{7}$$

The combination of (5) and (3) gives

$$\boldsymbol{\mu} = \boldsymbol{M}\boldsymbol{L}(\boldsymbol{q})\dot{\boldsymbol{q}} \tag{8}$$

Then, the equations of motion become a first order DAE system, with variables $\boldsymbol{q}$, $\boldsymbol{\mu}$ and $\boldsymbol{\lambda}$:

$$\begin{aligned} \boldsymbol{L}^T \dot{\boldsymbol{\mu}} + \frac{\partial \mathcal{V}}{\partial \boldsymbol{q}} + \boldsymbol{B}^T \boldsymbol{\lambda} + \dot{\boldsymbol{L}}^T \boldsymbol{\mu} - \frac{\partial}{\partial \boldsymbol{q}} \left[(\boldsymbol{L}\dot{\boldsymbol{q}})^T \boldsymbol{\mu} \right] &= \boldsymbol{0} \\ \boldsymbol{\mu} - \boldsymbol{M}\boldsymbol{L}(\boldsymbol{q})\dot{\boldsymbol{q}} &= \boldsymbol{0} \\ \boldsymbol{\Phi}(\boldsymbol{q}) &= \boldsymbol{0} \end{aligned} \tag{9}$$

where $\boldsymbol{B} = \partial\boldsymbol{\Phi}/\partial\boldsymbol{q}$ is the Jacobian matrix of constraints. Note that the last two terms in (9-a) can be written as

$$\dot{\boldsymbol{L}}^T\boldsymbol{\mu} - \frac{\partial}{\partial\boldsymbol{q}}\left[(\boldsymbol{L}\dot{\boldsymbol{q}})^T\boldsymbol{\mu}\right] = \boldsymbol{G}(\boldsymbol{\mu})\dot{\boldsymbol{q}} \tag{10}$$

where the matrix $\boldsymbol{G}(\boldsymbol{\mu})$ has the following components:

$$G_{jp} = \sum_i \mu_i \left(\frac{\partial L_{ij}}{\partial q_p} - \frac{\partial L_{ip}}{\partial q_j}\right) \tag{11}$$

Skew-symmetry of $\boldsymbol{G}$ follows immediately. The final form of the equations of motion is thus:

$$\begin{aligned} \boldsymbol{L}^T\dot{\boldsymbol{\mu}} + \frac{\partial\mathcal{V}}{\partial\boldsymbol{q}} + \boldsymbol{B}^T\boldsymbol{\lambda} + \boldsymbol{G}(\boldsymbol{\mu})\dot{\boldsymbol{q}} &= \boldsymbol{0} \\ \boldsymbol{\mu} - \boldsymbol{M}\boldsymbol{L}(\boldsymbol{q})\dot{\boldsymbol{q}} &= \boldsymbol{0} \\ \boldsymbol{\Phi}(\boldsymbol{q}) &= \boldsymbol{0} \end{aligned} \tag{12}$$

3 THE TIME CONTINUOUS GALERKIN APPROXIMATION: ENERGY PRESERVATION SCHEME

3.1 Discretization of the equation of motion

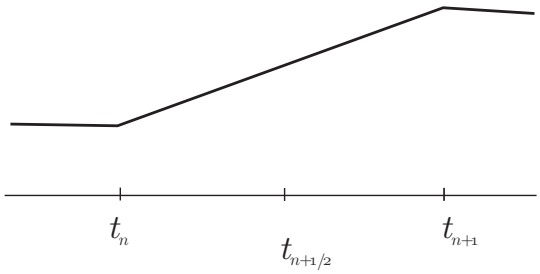

Figure 1: The time continuous Galerkin approximation of displacements and velocities

In the Galerkin approximation the equations of motion are enforced in a weak (integral) manner. The Galerkin approximation of the equations of motion (12) is written as

$$\begin{aligned} &\frac{h}{2}\int_{-1}^{1}\mathcal{W}_1(\tau)\left(\dot{\boldsymbol{q}} - \boldsymbol{L}^{-1}\boldsymbol{v}\right)d\tau + \\ &\qquad \frac{h}{2}\int_{-1}^{1}\mathcal{W}_2(\tau)\left(\boldsymbol{M}\dot{\boldsymbol{v}} + \boldsymbol{L}^{-T}\boldsymbol{G}\dot{\boldsymbol{q}} + \boldsymbol{L}^{-T}\frac{\partial\mathcal{V}}{\partial\boldsymbol{q}} + \boldsymbol{L}^{-T}\boldsymbol{B}^T\boldsymbol{\lambda}\right)d\tau = \boldsymbol{0} \end{aligned} \tag{13}$$

where $\mathcal{W}_i(\tau)$ are the weight functions, h is the time step size and τ a nondimensional time variable ($\tau = -1$ at t_n and $\tau = 1$ at t_{n+1}). By using piecewise linear interpolation functions for the displacements and velocities (Figure 1) and piecewise constant test functions $\mathcal{W}_1$ and $\mathcal{W}_2$, we obtain the set of discrete equations:

$$\begin{cases} \dfrac{1}{h}\boldsymbol{L}^T_{n+\frac{1}{2}}\boldsymbol{M}(\boldsymbol{v}_{n+1} - \boldsymbol{v}_n) + \dfrac{1}{h}\boldsymbol{G}_{n+\frac{1}{2}}(\boldsymbol{q}_{n+1} - \boldsymbol{q}_n) + \left.\dfrac{\partial\mathcal{V}}{\partial\boldsymbol{q}}\right|_{n+\frac{1}{2}} + \boldsymbol{B}^T_{n+\frac{1}{2}}\boldsymbol{\lambda}_{n+\frac{1}{2}} = \boldsymbol{0} \\ \dfrac{1}{h}\boldsymbol{L}_{n+\frac{1}{2}}(\boldsymbol{q}_{n+1} - \boldsymbol{q}_n) = \dfrac{1}{2}(\boldsymbol{v}_{n+1} + \boldsymbol{v}_n) \\ \boldsymbol{\Phi}_{n+1}(\boldsymbol{q}) = \boldsymbol{0} \end{cases} \tag{14}$$

The matrix $\boldsymbol{L}_{n+\frac{1}{2}}$ depends on the adopted rotation parametrization. The parametrization used (Euler parameters) assures a constant matrix $\boldsymbol{L}_{n+\frac{1}{2}}$ as it is shown in a previous work (Lens et al., 2004; Lens, 2006).

3.2 Energy preservation in the discrete scheme

The total energy of the system is $\mathcal{E}(\boldsymbol{q},\dot{\boldsymbol{q}}) = \mathcal{K}(\dot{\boldsymbol{q}}) + \mathcal{V}(\boldsymbol{q})$ where the kinetic energy has as a final expression $\mathcal{K} = \frac{1}{2}\boldsymbol{v}^T\boldsymbol{M}\boldsymbol{v}$ and the potential energy $\mathcal{V}(\boldsymbol{q})$ is a function of the generalized coordinates $\boldsymbol{q}$. The total energy change in a time step can be evaluated computing the work done by the elastic, constraint and inertia forces.
To prove the total energy preservation of the discrete scheme, we multiply (14-a) by the displacements jump $(\boldsymbol{q}_{n+1}-\boldsymbol{q}_n)^T$ over a time step

$$\frac{1}{h}(\boldsymbol{q}_{n+1}-\boldsymbol{q}_n)^T\boldsymbol{L}_{n+\frac{1}{2}}\boldsymbol{M}(\boldsymbol{v}_{n+1}-\boldsymbol{v}_n) + \frac{1}{h}(\boldsymbol{q}_{n+1}-\boldsymbol{q}_n)^T\boldsymbol{G}_{n+\frac{1}{2}}(\boldsymbol{q}_{n+1}-\boldsymbol{q}_n) + (\boldsymbol{q}_{n+1}-\boldsymbol{q}_n)^T\left.\frac{\partial\mathcal{V}}{\partial\boldsymbol{q}}\right|_{n+\frac{1}{2}} + (\boldsymbol{q}_{n+1}-\boldsymbol{q}_n)^T\boldsymbol{B}^T_{n+\frac{1}{2}}\boldsymbol{\lambda}_{n+\frac{1}{2}} = 0 \quad (15)$$

By looking at the first term we can identify the kinetic energy jump over a time step as:

$$\frac{1}{h}(\boldsymbol{q}_{n+1}-\boldsymbol{q}_n)^T\boldsymbol{L}_{n+\frac{1}{2}}\boldsymbol{M}(\boldsymbol{v}_{n+1}-\boldsymbol{v}_n) = \frac{1}{2}(\boldsymbol{v}_{n+1}+\boldsymbol{v}_n)^T\boldsymbol{M}(\boldsymbol{v}_{n+1}-\boldsymbol{v}_n) = \mathcal{K}_{n+1}-\mathcal{K}_n \quad (16)$$

Due to the skew-symmetry of the matrix $\boldsymbol{G}$ the second term becomes identically null.

$$\frac{1}{h}(\boldsymbol{q}_{n+1}-\boldsymbol{q}_n)^T\boldsymbol{G}_{n+\frac{1}{2}}(\boldsymbol{q}_{n+1}-\boldsymbol{q}_n) = \boldsymbol{0} \quad (17)$$

In the term of elastic forces derived from the potential $\mathcal{V}$, we substitute the derivative at the midpoint $(\partial\mathcal{V}/\partial\boldsymbol{q})_{n+\frac{1}{2}}$ by the approximation $(\partial\mathcal{V}/\partial\boldsymbol{q})^*_{n+\frac{1}{2}}$ (*discrete directional derivative*(Gonzalez, 1999)) that satisfies the condition:

$$(\boldsymbol{q}_{n+1}-\boldsymbol{q}_n)^T\left.\frac{\partial\mathcal{V}}{\partial\boldsymbol{q}}\right|^*_{n+\frac{1}{2}} = \mathcal{V}_{n+1}-\mathcal{V}_n \quad (18)$$

In the constraint forces term we use again the concept of *discrete directional derivative* where now the Jacobian matrix of constraints $\boldsymbol{B}_{n+\frac{1}{2}}$ is replaced by the approximation $\boldsymbol{B}^*_{n+\frac{1}{2}}$ in order to satisfy

$$(\boldsymbol{\Phi}_{n+1}-\boldsymbol{\Phi}_n) = \boldsymbol{B}^*_{n+\frac{1}{2}}(\boldsymbol{q}_{n+1}-\boldsymbol{q}_n) \quad (19)$$

With this condition,

$$(\boldsymbol{q}_{n+1}-\boldsymbol{q}_n)^T\boldsymbol{B}^{*T}_{n+\frac{1}{2}}\boldsymbol{\lambda}_{n+\frac{1}{2}} = (\boldsymbol{\Phi}_{n+1}-\boldsymbol{\Phi}_n)\,\boldsymbol{\lambda}_{n+\frac{1}{2}} \quad (20)$$

The configuration at time t_n is assumed to be compatible, $\boldsymbol{\Phi}_n = \boldsymbol{0}$. Then, forcing

$$\boldsymbol{\Phi}_{n+1} = \boldsymbol{0} \quad (21)$$

we guarantee that the work of the constraints forces is zero.
By replacing equations (16), (17), (18) and (19) into equation (15) we may see that the total energy change of the system over a time step results

$$\mathcal{E}_{n+1}-\mathcal{E}_n = \mathcal{K}_{n+1}-\mathcal{K}_n+\mathcal{V}_{n+1}-\mathcal{V}_n = 0 \quad (22)$$

Therefore, the scheme formed by the equation set (14) preserves the total energy of the system if (18), (19) and (21) are satisfied.

4 CONTACT CONDITION

In this section two different types of contact problems will be addressed. At first, the contacting bodies are assumed to be infinitely rigid, giving rise to the inequality condition $q \geq 0$. Next, the bodies are assumed to be deformable under hypothesis of small deformations. At contact, a new variable a is introduced. This quantity is defined as the *approach* and when inter-penetration occurs we have $a > 0$ and $q < 0$. Without inter-penetration we have that $a = 0$ and $q > 0$. By combining both situations we arrive to the contact condition $q + a \geq 0$, which implies $q = -a$ for the case of inter-penetration. For this case, a suitable phenomenological model for the contact forces as function of the approach between contact bodies must be taken into account. The magnitude of a will depend on the chosen potential contact model. A schematic plot of q and a with and without inter-penetration is shown in Figure 2

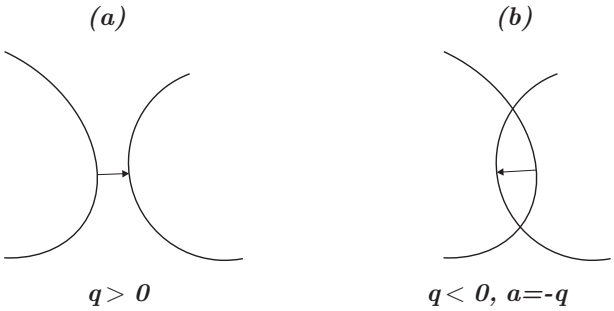

Figure 2: (a) non inter-penetration case: $a = 0$ and $q > 0$. (b) inter-penetration case : $q = -a$

4.1 Rigid Impact Between Bodies

The contact condition for rigid impact between two bodies is an inequality $q \geq 0$ which can be transformed into an equality condition $q - r^2 = 0$ through the addition of a slack variable r. Hence, the contact condition is enforced as a nonlinear holonomic constraint

$$\Phi = q - r^2 = 0 \tag{23}$$

The constraint forces arise from

$$\delta\Phi\lambda = \begin{bmatrix}\delta q \\ \delta r\end{bmatrix}^T \begin{bmatrix}\lambda \\ -2\lambda r\end{bmatrix} \tag{24}$$

and are discretized in such a way that the work they perform vanishes over a time step. The discrete forces are expressed as

$$\begin{bmatrix}\lambda_{n+\frac{1}{2}} \\ -2\lambda_{n+\frac{1}{2}} r_{n+\frac{1}{2}}\end{bmatrix} \tag{25}$$

where $r_{n+\frac{1}{2}} = (r_{n+1} + r_n)/2$. The work done by the discretized forces of constraint is computed as $(\Phi_{n+1} - \Phi_n)\lambda_{n+\frac{1}{2}}$. In a similar manner as it was done in Section 3.2, by enforcing $\Phi_{n+1} = 0$ the vanishment of the discrete work and the avoidance of the drift phenomenon are guaranteed.

Since the slack variable is not connected to any degree of freedom of the model, the variation δr gives rise to the non linear equation $-2\lambda_{n+\frac{1}{2}} r_{n+\frac{1}{2}} = 0$ which possesses two solutions. The first one, $\lambda_{n+\frac{1}{2}} = 0$ is asociated to the non contact condition. The second one, $r_{n+\frac{1}{2}} = 0$ indicates an active contact condition and implies $r_{n+1} = -r_n$, which together with $\Phi_{n+1} = \Phi_n = 0$

results in $q_{n+1} = r_{n+1}^2 = r_n^2 = q_n$. In other words, when the contact condition is activated, a contact force $\lambda_{n+\frac{1}{2}} \neq 0$ is developed and the relative distance between the contacting bodies remains unchanged. Finally, the relationship between velocities and displacements given by equation (14-b):

$$\frac{\dot{q}_{n+1} + \dot{q}_n}{2} = \frac{q_{n+1} - q_n}{h} \tag{26}$$

which yields $\dot{q}_{n+1} = \dot{q}_n$. For further details, see reference (Bauchau, 2000).

4.2 Flexible Impact Between Bodies

When we consider the contact as flexible, the contact condition becomes $q + a \geq 0$ where a is the quantity defined as the *approach* between bodies. A suitable phenomenological model for the contact forces expressed as function of the approach between the contact bodies must be introduced. In this work we will adopt an elastic potential by using a piecewise linear contact force like that plotted in Figure 3. As discussed in section 3.2, the expression of the elastic

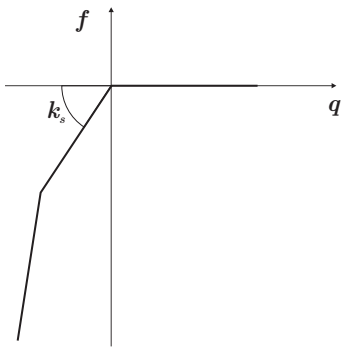

Figure 3: Elastic potential: piecewise linear contact force

forces for the energy preserving integration scheme must satisfy the condition established by equation (18):

$$(q_{n+1} - q_n) \left.\frac{\partial \mathcal{V}}{\partial q}\right|_{n+\frac{1}{2}}^{*} = \mathcal{V}_{n+1} - \mathcal{V}_n \tag{27}$$

where the potential $\mathcal{V}(q)$ has for expression

$$\mathcal{V} = \int_{q_0}^{q} f(q)dq + \mathcal{V}_0 \tag{28}$$

hence the elastic force expression for the energy preserving scheme writes

$$\left.\frac{\partial \mathcal{V}}{\partial q}\right|_{n+\frac{1}{2}}^{*} = \frac{\int_{q_0}^{q_{n+1}} f(q)dq - \int_{q_0}^{q_n} f(q)dq}{q_{n+1} - q_n} = \frac{\int_{q_n}^{q_{n+1}} f(q)dq}{q_{n+1} - q_n} \tag{29}$$

By computing the derivative of this expression with respect of $q_{n+\frac{1}{2}}$, we obtain the stiffness contribution as:

$$K = 2\frac{f(q_{n+1})(q_{n+1} - q_n) - \int_{q_n}^{q_{n+1}} f(q)dq}{(q_{n+1} - q_n)^2} = 2\frac{f(q_{n+1}) - \left.\frac{\partial \mathcal{V}}{\partial q}\right|_{n+\frac{1}{2}}^{*}}{(q_{n+1} - q_n)} \tag{30}$$

5 NUMERICAL EXAMPLES

In this section we present several examples of rigid and flexible impact between rigid and flexible bodies, to show the performance of the proposed algorithm. The beam model used in this paper is documented in (Lens and Cardona, 2007; Lens, 2006). The unconditional stability of the integration scheme is guaranteed by the element formulation, by providing the energy preservation at each time step.

5.1 Two rigid pendulums with mutual rigid impact

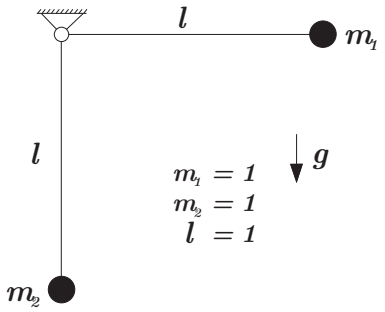

Figure 4: Two pendulums with mutual impact

Figure 4 shows the problem of impact between two pendulums of unit mass and length. The problem has four degrees of freedom $\boldsymbol{q}^T = [x_1 \quad x_2 \quad y_1 \quad y_2]$, and is subjected to two length constraints $\Phi_1 = x_1^2 + y_1^2 - \ell^2 = 0$ and $\Phi_2 = x_2^2 + y_2^2 - \ell^2 = 0$, and the intermittent contact constraint. The right pendulum is dropped from its horizontal position with zero initial velocity. Contact was modelled using the rigid impact approach of section 4.1. Figure 5 displays the

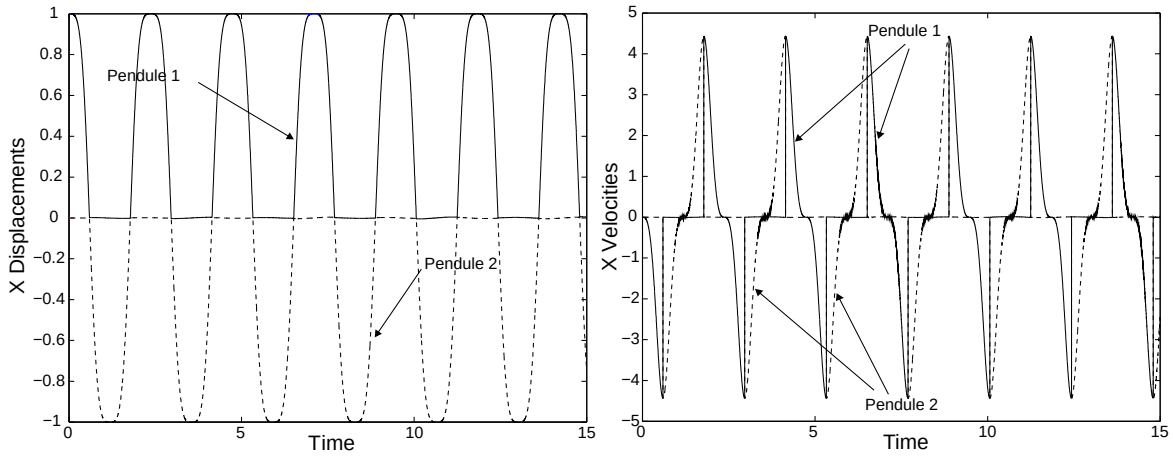

Figure 5: Displacements and velocities vs. time - X coordinate

time history of displacements and velocities for both bodies, where it can be seen once again that the periodic character is perfectly preserved. Figure 6 shows that for this example the scheme verifies first order accuracy, although the integration scheme is second order accurate for standard problems. This loss of accuracy is caused by the rigid impact modelling.

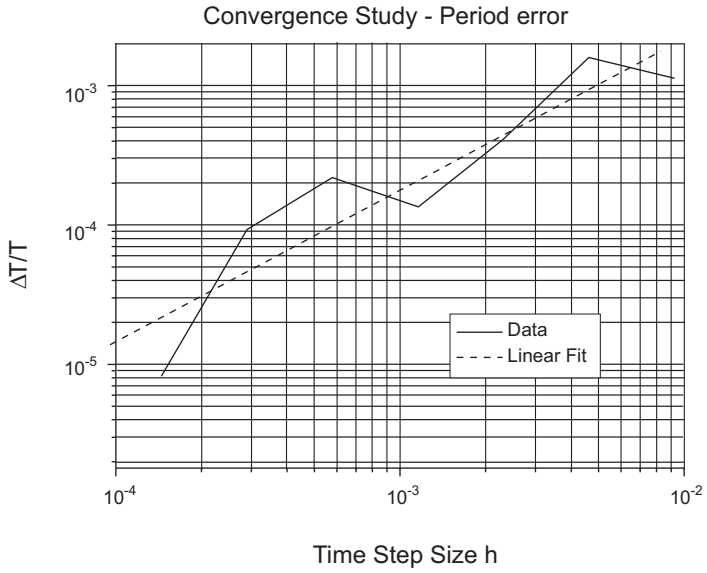

Figure 6: Two pendulums mutual impact: convergence study

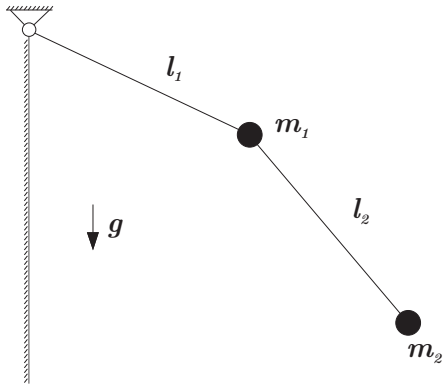

Figure 7: Double pendulum against a rigid wall

5.2 Double Rigid Pendulum Impacting a Rigid Wall

This example deals with a double pendulum that impacts against a rigid wall (Figure 7, $m_1 = m_2 = 1$ kg and $\ell_1 = \ell_2 = 1$ m). The system is dropped from its horizontal position with zero initial velocities. The simulation results are displayed in Figures 8 and 9, for a time step size of 0.0005 s. The impact can be clearly identified as a discontinuity in the displacements and a jump in the velocities.

5.3 Impact of a Simple Pendulum on a Rigid Stop

The last example deals with the impact of a simple pendulum on a rigid stop. To model the pendulum, two alternatives were taken into account: (a) a rigid body model and (b) a flexible beam model. The pendulum is 1 m long and is subjected to the action of the gravitational field. The mass of the rigid body is $m = 0.25$ kg. The beam data is: section area $A = 0.0005\ \mathrm{m}^2$, section inertias $I_x = 2 \times 10^{-7}\ \mathrm{m}^4$ and $I_y = I_z = 1 \times 10^{-7}\ \mathrm{m}^4$, elastic modulus $E = 2.1 \times 10^{11}\ \mathrm{N/m}^2$, mass density $\rho = 7800\ \mathrm{kg/m}^3$ and Poisson modulus $\nu = 0.3$. The pendulum was modelled using 10 beam elements. Figure 10 shows schematic draws of both models. The initial condition is depicted in the figure, i.e. the pendulum is dropped from its

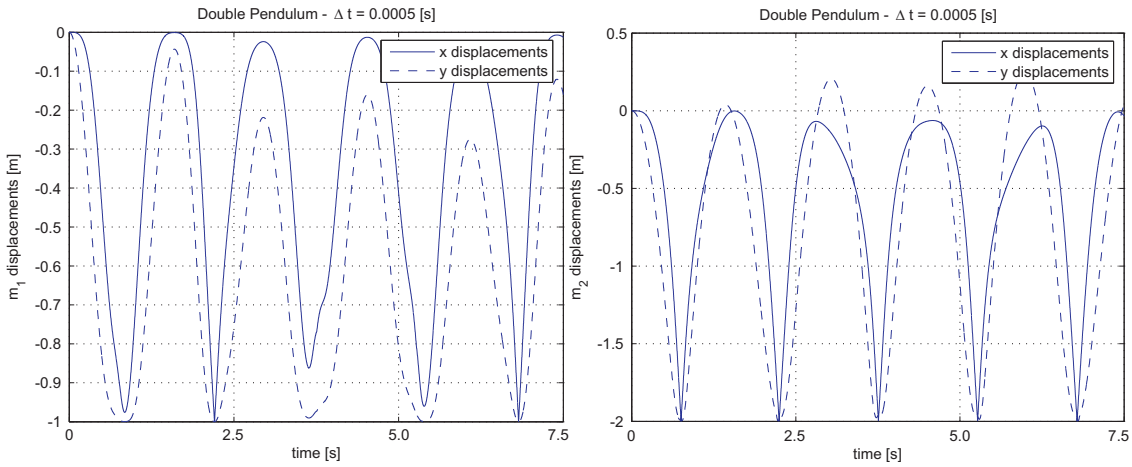

Figure 8: Double pendulum: x and y displacements for (a) m_1 and (b) m_2

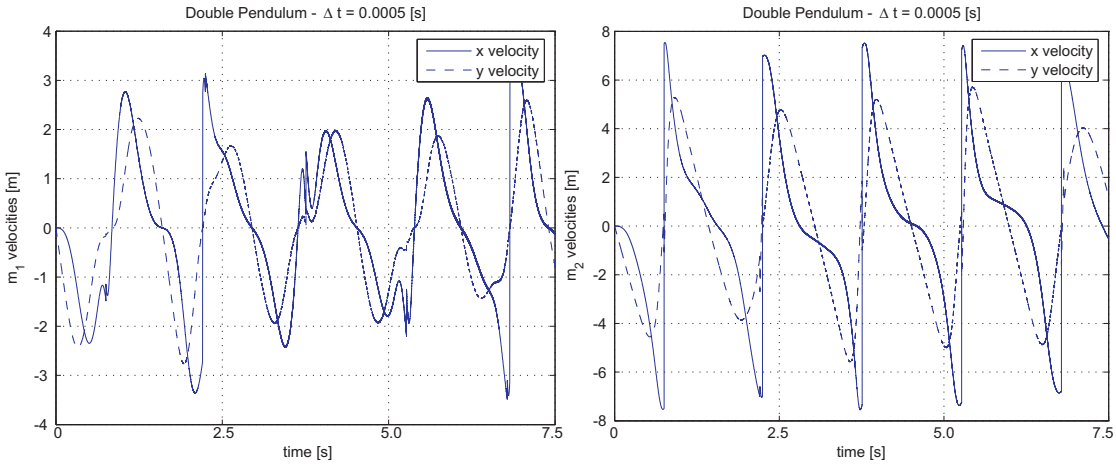

Figure 9: Double pendulum: x and y velocities for (a) m_1 and (b) m_2

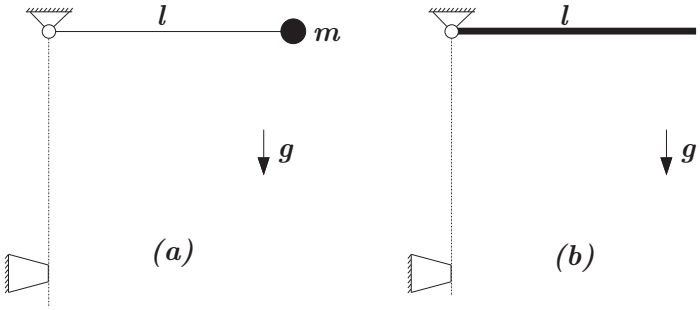

Figure 10: Impact of a simple pendulum on a rigid stop: (a) rigid body and (b) beam model

horizontal position with zero initial velocity. All results displayed in this section are for a time step size $\Delta t = 0.000006$ s.

Figure 11-a shows the time response of displacements x and y of the mass m for the rigid body case. It can be seen that after the impact the mass returns to the point of depart $y = 0$ due to the energy preservation that is shown in Figure 11-b.

For the case of the beam model we analyzed both contact alternatives: the rigid and the flexible impact, as described in sections 4.1 and 4.2. Several tests were performed for different time

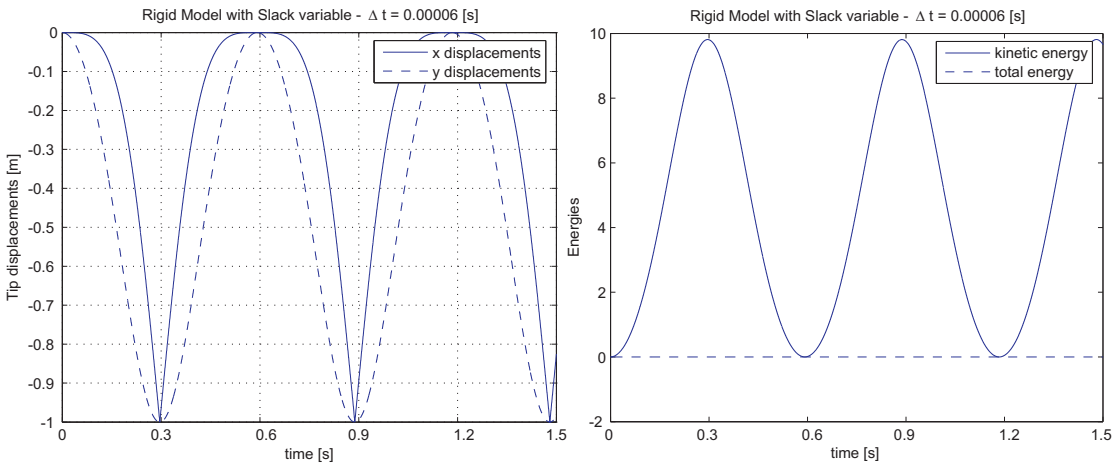

Figure 11: Rigid body model: (a) x and y tip displacements and (b) energy preserving

step sizes and for different values of the constant stiffness k_s. Figure 12 shows the x and y displacements of the tip of the beam, for (a) the rigid impact model with the slack variable and (b) the flexible contact model with the piecewise linear contact force. The value of the contact stiffness for this case is $k_s = 1 \times 10^8$ N/m^2, the highest value of contact stiffness used in all tests. We can see that for the first impact both responses are very similar but after the second impact they show very different behaviours.

We would like to note that in the case of using the flexible impact model, the computed responses converged to a solution for decreasing values of time step size. On the other hand, when using the slack variable approach, the responses computed after the second impact displayed a chaotical behaviour for varying values of time step size.

Very rapid vibration oscillations are excited in the beam after the first impact, as can be seen

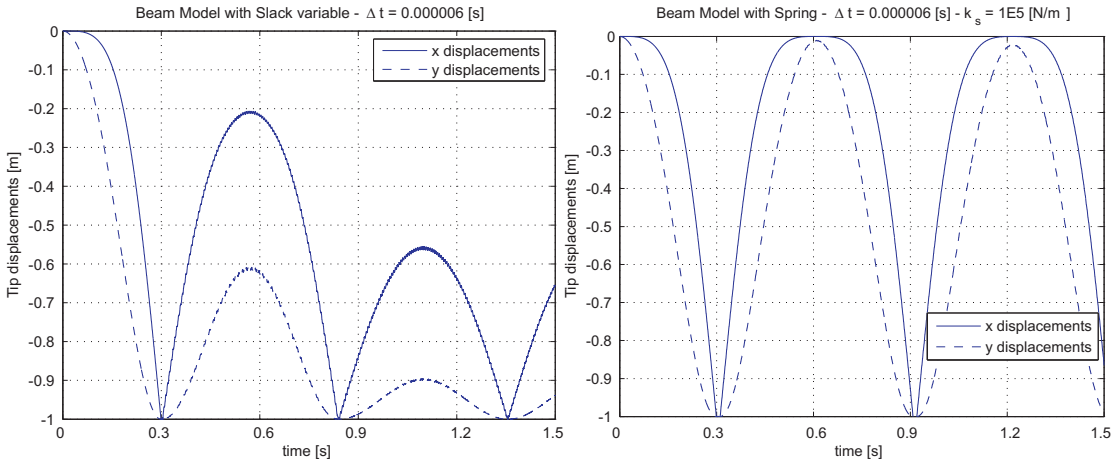

Figure 12: Beam model: x and y displacements for both models of impact (a) rigid (b) flexible with $k_s = 1 \times 10^8$ N/m

in Figures 14-16. For this reason, the tip of the beam is rapidly oscillating at the time of approaching the stop at second impact, and the computation of motion after impact may present very different responses, especially in the case of using the rigid contact model.

By using the penalty approach, the problem is regularized and we observe a small dependence of the results on the time step size. It can be seen that the beam model response converge to

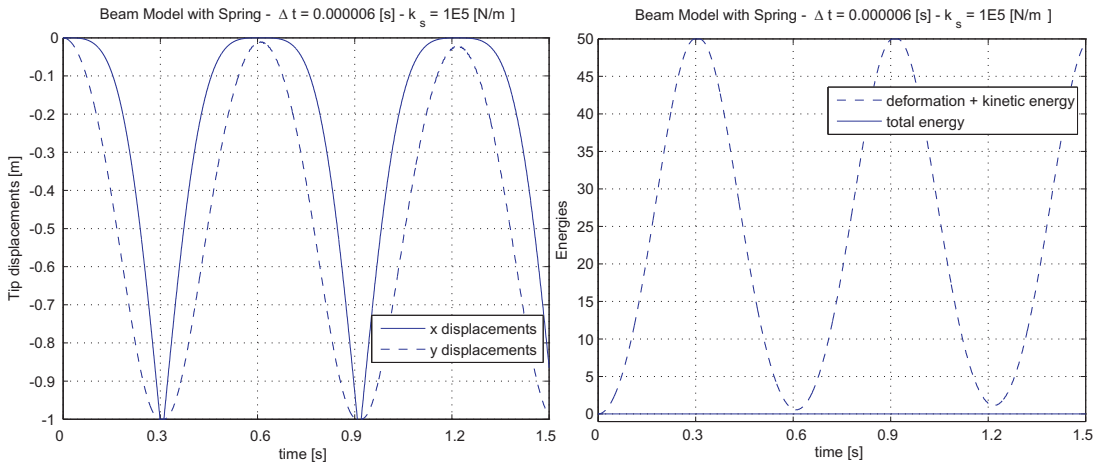

Figure 13: Beam model: (a) x and y tip displacements and (b) energy preserving for the flexible impact model with $k_s = 1 \times 10^5$ N/m

the rigid body response when decreasing the value of the k_s coefficient (Figure 13), since the excited beam oscillations are smaller in this case.

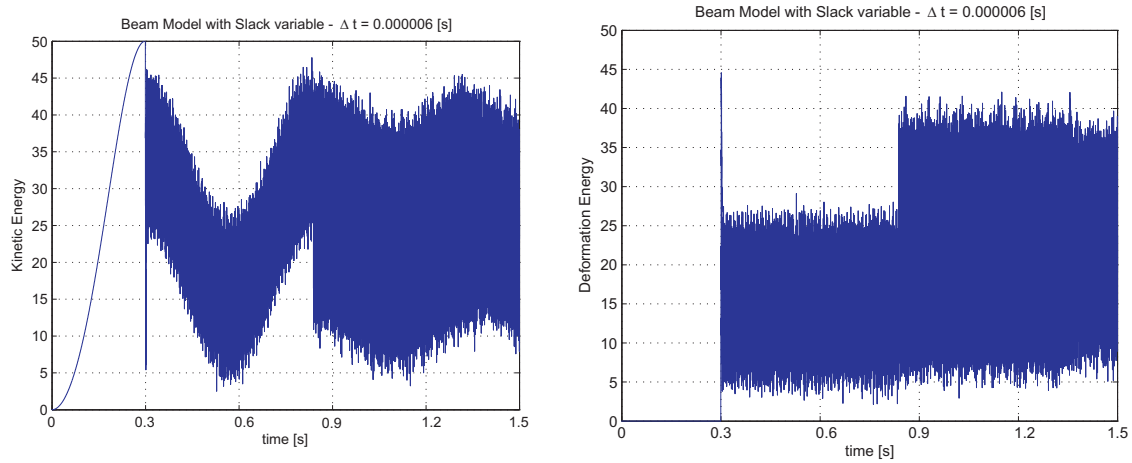

Figure 14: Beam model: (a) kinetic energy and (b) deformation energy for the rigid impact model.

6 CONCLUSIONS

A methodology for nonlinear, flexible multibody systems undergoing intermittent contact has been presented. Contact duration is assumed finite and the contact force is computed in an explicit way as part of the simulation.

The unilateral contact condition is transformed into a holonomic constraint by using a slack variable, in the case of rigid impact model. When the impact is considered as flexible, a simple model relating contact forces and the inter-penetration was used.

It was observed that the rigid contact model does work fine for intermittent contact between rigid bodies only. When we tried to use this model with deformable bodies, the results obtained did not converge to a solution. The best results for flexible bodies were obtained using the flexible impact model.

Several numerical examples were presented to illustrate the performance of the analyzed methodologies.

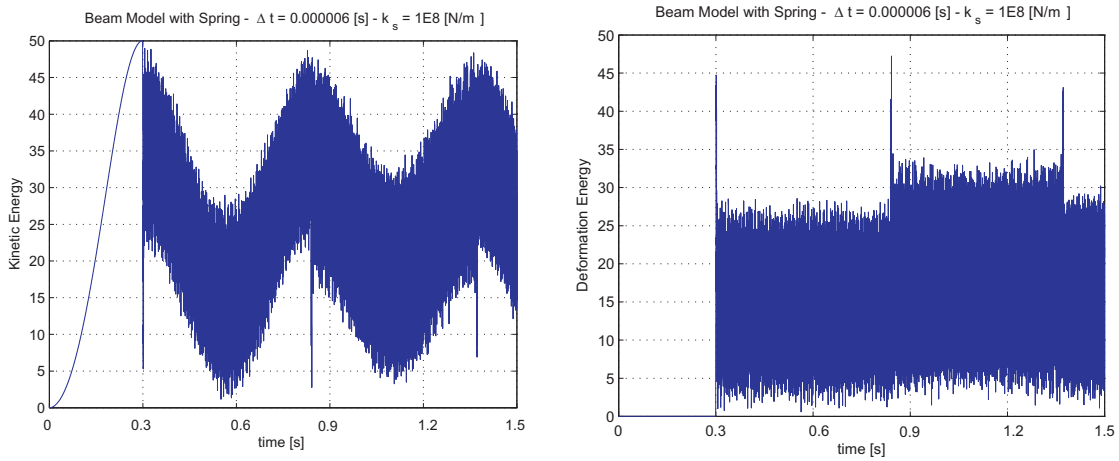

Figure 15: Beam model: (a) kinetic energy and (b) deformation energy for the flexible impact model, with $k_s = 1 \times 10^8$ N/m.

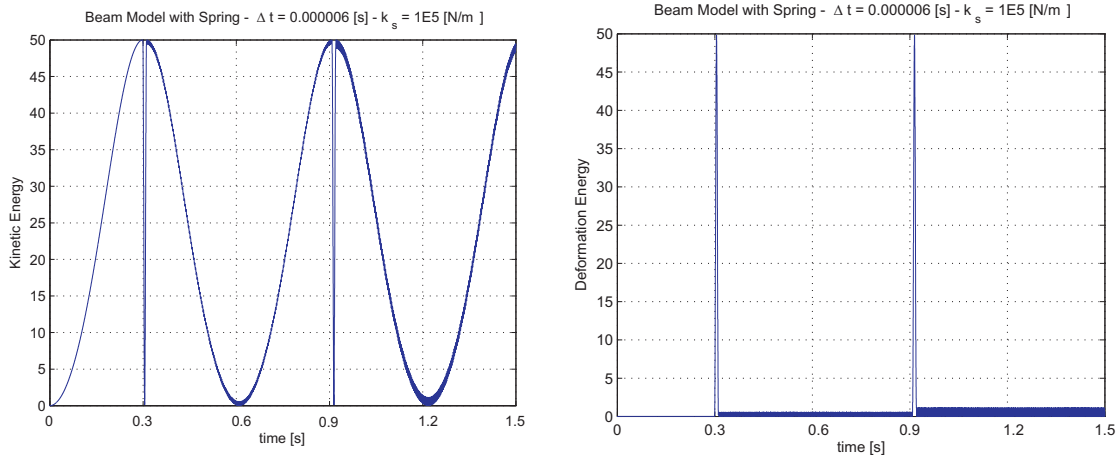

Figure 16: Beam model: (a) kinetic energy and (b) deformation energy for the flexible impact model, with $k_s = 1 \times 10^5$ N/m.

REFERENCES

Bauchau O. Analysis of flexible multibody systems with intermittent contacts. *Multibody System Dynamics*, 4:23–54, 2000.

Bottasso C.L. and Trainelli L. Implementation of effective procedures for unilateral contact modelling in multibody dynamics. *Mechanics Research Communications*, 28(3):233–246, 2001.

Gonzalez O. Mechanical systems subject to holonomic constraints: differential-algebraic formulations and conservative integration. *Physica D*, 132:165–174, 1999.

Kane T.R. Impulsive motions. *Journal of Applied Mechanics*, 15:718–732, 1962.

Khulief Y.A. and Shabana A.A. Dynamic analysis of constrained systems of rigid and flexible bodies with intermittent motion. *ASME Journal of Mechanisms, Transmissions and Automation in Design*, 108:38–44, 1986.

Lens E. *Energy Preserving/Decaying Time Integration Schemes for Multibody Systems Dynamics*. Ph.D. thesis, Universidad Nacional del Litoral, Argentina, 2006.

Lens E. and Cardona A. A nonlinear beam element formulation in the framework of an energy preserving time integration scheme for constrained multibody system dynamics. *Computers*

and structures, 2007. In press.

Lens E., Cardona A., and Géradin M. Energy preserving time integration for constrained multibody systems. *Multibody System Dynamics*, 11:41–61, 2004.

Pfeiffer F. and Glocker C. *Multibody Dynamics with Unilateral Contacts*. John Wiley & Sons Inc., New York, NY, 1996.